

Circuit Coupling Model Containing Equivalent Eddy Current Loss Impedance for Wireless Power Transfer in Seawater

Wangqiang Niu, Chen Ye, Wei Gu

Key Laboratory of Transport Industry of Marine Technology and Control Engineering,
Shanghai Maritime University,
Shanghai, 201306
China

Received: November 2, 2020. Revised: April 1, 2021. Accepted: April 19, 2021. Published: April 23, 2021.

Abstract- Nowadays, as the whole world put more emphasis on ocean resource exploration, the use of automatic underwater vehicles (UAVs) comes to be increasingly frequent. Inductive wireless power transfer (IWPT), as a power transfer solution with high safety and flexibility, is quite promising applied in UAV power supply. However, when applied underwater, IWPT efficiency decreases due to eddy current loss (ECL) caused by high conductivity of water medium. In order to analyze IWPT output characteristics in seawater, this paper proposes a coupling circuit model involving equivalent eddy current loss impedance (EECLI), which is derived via three-coil model. On the one hand, it is found that splitting frequency still exists in IWPT under seawater. On the other hand, EECLI is independent to coil distance, but proportional to operation frequency. The validity of the proposed model for IWPT system with coils in small size (coil outer diameter 12 cm, system resonant frequency 570 kHz) is verified by experiment, which means it is available for IWPT system design and analysis.

Keywords- inductive wireless power transfer, equivalent eddy current loss impedance, coupling circuit model, frequency splitting, resonant circuit in series.

I. INTRODUCTION

WITH the great development of electric and electronic equipment age, people now have much higher requirements on electric power transmission scenarios, particularly for those mobile electrical appliances which need to work sustainably for a long time and are limited by battery performance [1–3]. Then, inductive wireless power transfer technology seems to be an ideal solution. Especially when applied in underwater automatic vehicle (UAV), inductive wireless power transfer has much better safety, flexibility and reliability than

traditional wired power transfer since high conductivity and corrosiveness in water environment may cause damage to charging interface [4].

However, water environments with different conductivity inevitably cause eddy current loss (ECL) and reduce IWPT efficiency [5]. Thus, it is valuable to explore effects of high conductivity of seawater on IWPT. [6] investigates WPT characteristics in air, pipe water and seawater by experiment, finding that to coils with large radius (decimeter level), both pipe water and seawater have significant attenuation effect on IWPT, even that frequency splitting phenomenon disappears compared to IWPT in air. Besides, when transmission distance keeps increasing and exceeds a certain value, the output voltage in liquid medium bounces back and trends to be a stable value which is much higher than output in air. Similarly, [7] reports the results of experiments addressing the effects of seawater conductivity on IWPT. Nevertheless, these researches lack theoretical details. As for frequency splitting in air, a common phenomenon to IWPT system with high quality factor, is discussed thoroughly in [8], but frequency splitting characteristics underwater is still in blank.

In order to further research IWPT underwater, theoretical analysis based on electromagnetic field (EMF) calculation was proposed by researchers. In [9], ECL in underwater IWPT is analyzed by EMF theory and parameter optimization impedance of IWPT system in seawater is proposed as well. Specially, equivalent eddy current loss (EECLI) is introduced into circuit model to simplify calculation procedure. While in [10], both ECL and detuning effect of seawater on IWPT are investigated. Moreover, the detuned system caused by seawater conductivity is turned back to resonance through adding a compensation inductance. Furthermore, [11] proposes ECL analysis of underwater WPT system with coil misalignments via geometry relation and Maxwell's equation. On the other hand, ECL can be reduced through frequency optimization as well [12].

Nevertheless, plain EECLI model mentioned previously is much too complex on calculation and lacks intuitiveness on physical explanation. [13] applies a model re-

garding medium with high conductivity as a relay circuit in eddy current testing (ECT). It also reveals that the medium with high conductivity reduces self-inductance on transmission side (Tx) and receiving side (Rx) increasing the resonance frequency.

In terms of underwater WPT designing, some work has been done considering UAV application. E.g., a new coil structure of $1 \times 1 \times 1$ is proposed in [14] to reduce eddy current loss of WPT systems for UAV. In this research, the receiving coil is set between two parallel transmitting coils and both simulation and experiment prove that the new structure can effectively reduce ECL in the field. [15] proposes a voltage output stabilization realized by integral circuit, which significantly reduces system volume while a good voltage stabilizing effect is guaranteed.

In this paper, a new WPT circuit model containing EECLI based on three-circuit model is proposed which is suitable for WPT system with small coils where inductance variation can be ignored. In order to prove the validity of the new model, WPT experiment in air and seawater is carried out. In the experiment, the output voltage is observed under various frequency and coil distance. It is found that frequency splitting exists both in air and seawater with little resonant frequency deviation. Meanwhile, the influence of EECLI on IWPT in seawater mainly occurs on the ridge of splitting. Furthermore, it is also found that EECLI has nothing to do with coil distance, but is proportional to operation frequency. The new model is conducive to simplify analysis and optimize design of IWPT in seawater compared with EMF model. Our techniques can be combined with similar studies in Electrical Engineering like [16–18].

II. CIRCUIT MODEL ANALYSIS FOR IWPT IN SEAWATER

In this section, a calculation model for IWPT in seawater based on three-coil circuit model is established first. Then, in order to evaluate EECLI caused by seawater, the equivalent relay circuit is mapped into EECLI in primary and second side by formula derivation.

A. Three-coil model

Different from IWPT in air, it is found that various extent of output attenuation usually occurs in IWPT underwater due to different conductivity of liquid medium or coil dimensions. In this paper, we assume that both Tx and Rx coils have a coupling effect with seawater medium, not only with each other. As a result, three-coil circuit model is introduced to analyze the output characteristics of IWPT in seawater as shown in Fig. 1. In this model, the equivalent seawater relay circuit consists of equivalent seawater resistor r_{sea} , inductor L_{sea} , mutual inductance M_{sea} with Tx and Rx coils which is equal. In primary side, U_s is AC voltage source, while L_1 and L_2 represent the inductance of Tx and Rx coil. M means the mutual inductance between Tx and Rx coils in air, which can be expressed as $k\sqrt{L_1 L_2}$ where k is the coupling coefficient. To make the system resonant at a certain frequency, two capacitors are connected into primary and second side in series, whose capacitance is

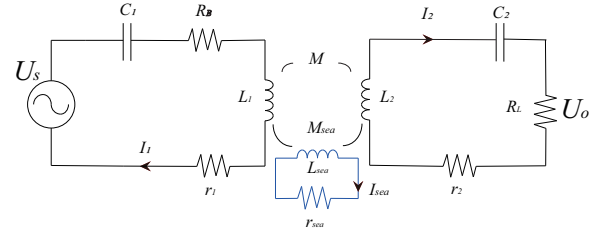


Fig. 1: The equivalent three-coil circuit model for IWPT in seawater

represented by C_1 and C_2 , separately. In addition, R_L is the load resistance, while R_B is the resistance set for balance, which means $R_L = R_B$ here. r_1 and r_2 denote coil internal resistance in primary and second side respectively. \mathbf{I}_1 , \mathbf{I}_2 and \mathbf{I}_{sea} represent the current flowing through Tx, Rx and equivalent seawater loop, respectively.

According to Kirchhoff's law (KVL), three loops are able to list three equations which are expressed as following matrix:

$$\begin{pmatrix} U_s \\ 0 \\ 0 \end{pmatrix} = \begin{pmatrix} Z_1 & -j\omega M & -j\omega M_{sea} \\ -j\omega M & Z_2 & j\omega M_{sea} \\ -j\omega M_{sea} & j\omega M_{sea} & Z_{sea} \end{pmatrix} \begin{pmatrix} \mathbf{I}_1 \\ \mathbf{I}_2 \\ \mathbf{I}_{sea} \end{pmatrix} \quad (1)$$

where Z_1 , Z_2 and Z_{sea} represent the equivalent impedance in three loops, respectively, of which expressions are given as: $Z_1 = R_B + r_1 + j(\omega L_1 - \frac{1}{\omega C_1})$, $Z_2 = R_L + r_2 + j(\omega L_2 - \frac{1}{\omega C_2})$ and $Z_{sea} = r_{sea} + j\omega L_{sea}$, while ω is the angular frequency. In order to obtain the theoretic EECLI, it is necessary to further transform (1). Solving the equations, the eddy current in seawater is expressed as

$$\mathbf{I}_{sea} = \frac{j\omega M_{sea}}{Z_{sea}} \mathbf{I}_1 - \frac{j\omega M_{sea}}{Z_{sea}} \mathbf{I}_2 \quad (2)$$

Then, we have

$$\begin{aligned} U_s &= Z_1 \mathbf{I}_1 - j\omega M \mathbf{I}_2 - j\omega M_{sea} \left(\frac{j\omega M_{sea}}{Z_{sea}} \mathbf{I}_1 - \frac{j\omega M_{sea}}{Z_{sea}} \mathbf{I}_2 \right) \\ \rightarrow U_s &= \left(Z_1 + \frac{(\omega M_{sea})^2}{Z_{sea}} \right) \mathbf{I}_1 - j\omega \left(M - M_{sea} \frac{j\omega M_{sea}}{Z_{sea}} \right) \mathbf{I}_2 \end{aligned} \quad (3)$$

In (3), the expression above can be divided into two parts, which is similar to coupling circuit without relay circuit. Thus, the first part and second part can be regarded as the new impedance of the primary side and second side respectively, while the equivalent relay circuit is eliminated. Further, we can get the new impedance of Tx coil expression as

$$\begin{aligned} Z_{Tx_{new}} &= r_{1_{new}} + j\omega L_{1_{new}} \\ &= r_1 + j\omega L_1 + \frac{(\omega M_{sea})^2 (r_{sea} - j\omega L_{sea})}{r_{sea}^2 + (\omega L_{sea})^2} \end{aligned} \quad (4)$$

$$\rightarrow r_1 + \frac{(\omega M_{sea})^2 r_{sea}}{r_{sea}^2 + (\omega L_{sea})^2} + j\omega \left(L_1 - \frac{(\omega M_{sea})^2 L_{sea}}{r_{sea}^2 + (\omega L_{sea})^2} \right) \quad (5)$$

The same deriving procedure can be adopted to obtain the new impedance expression in the second side as following

$$\begin{aligned} Z_{R_{x_{new}}} &= r_{2_{new}} + j\omega L_{2_{new}} \\ &= r_2 + \frac{(\omega M_{sea})^2 r_{sea}}{r_{sea}^2 + (\omega L_{sea})^2} + j\omega \left(L_2 - \frac{(\omega M_{sea})^2 L_{sea}}{r_{sea}^2 + (\omega L_{sea})^2} \right) \end{aligned} \quad (6)$$

From (5) and (6), the new impedance and inductance on two sides can be summed up as following

$$r_{i_{new}} = r_i + \frac{(\omega M_{sea})^2 r_{sea}}{r_{sea}^2 + (\omega L_{sea})^2} \quad (7)$$

and

$$L_{i_{new}} = L_i - \frac{(\omega M_{sea})^2 L_{sea}}{r_{sea}^2 + (\omega L_{sea})^2} \quad (8)$$

where $i = 1, 2$ representing original impedance and inductance on primary and second side respectively. Through analysis on three-coil model for WPT in seawater, it can be seen that theoretically seawater has influence on both impedance and inductance in WPT system. For impedance and inductance, they respectively increase and reduce certain value which is relative with the M_{sea} , L_{sea} , r_{sea} and ω , meanwhile the value of the former three parameters are dependent on coil dimension and seawater characteristics, e.g., conductivity, permittivity and permeability. In this case, the L_{sea} is quite tiny because the corresponding coil dimension is small. Thus, we ignore the variation of coil inductance.

B. Equivalent eddy current loss impedance model

In order to analyze seawater attenuation effect on WPT, the concept of equivalent eddy current loss impedance R_{eddy} is usually introduced. In [10], first the electric field intensity E is obtained by EMF calculation and then the eddy current loss can be derived as $P_{eddy} = \iiint_V \sigma E^2 dV$, where V is the volume of ECL and σ is the conductivity of seawater. Finally, the value of EECLI is gained by the equation $R_{eddy} = P_{eddy}/I$ where I is the current in coil.

However, EMF methodology involves integration to the square of Bessel function, which increases the complexity of calculation. In this paper, different from EMF methodology, the proposed EECLI model is derived by pure coupling circuit model, which is much more intuitive. From (7), the expression of EECLI can be extracted as

$$R_{eddy} = \frac{(\omega M_{sea})^2 r_{sea}}{r_{sea}^2 + (\omega L_{sea})^2} \quad (9)$$

In this case, to simplify the EECLI model, we assume that r_{sea} is proportional to ω , namely $r_{sea} = \alpha\omega$, where α is defined as resistance coefficient in seawater, thus the expression of R_{eddy} can be further transformed as

$$R_{eddy} = \frac{M_{sea}^2 \alpha}{\alpha^2 + L_{sea}^2} \omega \quad (10)$$

It can be seen that the value of R_{eddy} is proportional to ω and we can consider $\frac{M_{sea}^2 \alpha}{\alpha^2 + L_{sea}^2}$ as a whole EECLI

coefficient β . Then R_{eddy} can be expressed as

$$R_{eddy} = \beta\omega \quad (11)$$

Thus, a new circuit model containing EECLI can be obtained as shown in Fig. 2, which is transformed from three-coil model. According to KVL, two loops can list two equations as following matrix:

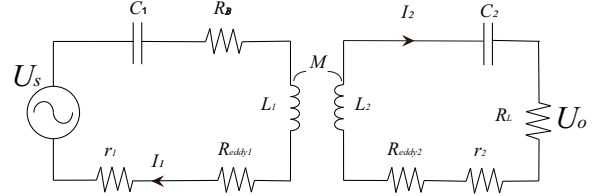


Fig. 2: The two-coil model containing equivalent eddy current loss impedance

$$\begin{pmatrix} U_s \\ 0 \end{pmatrix} = \begin{pmatrix} Z_1 + R_{eddy1} & -j\omega M \\ -j\omega M & Z_2 + R_{eddy2} \end{pmatrix} \begin{pmatrix} \mathbf{I}_1 \\ \mathbf{I}_2 \end{pmatrix} \quad (12)$$

Thus, we can get complete circuit equations as below:

$$\begin{cases} U_s - (r_1 + R_{eddy1} + R_B + j\omega L_1 + \frac{1}{j\omega C_1}) \mathbf{I}_1 = j\omega M \mathbf{I}_2 \\ \mathbf{I}_2 (r_2 + R_{eddy2} + R_L + j\omega L_2 + \frac{1}{j\omega C_2}) = -j\omega M \mathbf{I}_1 \end{cases} \quad (13)$$

where $\mathbf{I}_1 = \frac{\mathbf{U}_{R_B}}{R_B}$ and $\mathbf{I}_2 = \frac{\mathbf{U}_o}{R_L}$, where \mathbf{U}_{R_B} is the voltage on R_B . Then the other expression of R_{eddy} can be derived as

$$\begin{cases} R_{eddy1} = \left| \frac{R_B (R_L U_s - j\omega \mathbf{U}_o)}{\mathbf{U}_{R_B} R_L} - Z_1 \right| \\ R_{eddy2} = \left| -j\omega M \frac{R_L \mathbf{U}_{R_B}}{R_1 \mathbf{U}_o} - Z_2 \right| \end{cases} \quad (14)$$

in order to verify theoretical value of R_{eddy} since the phase and amplitude of \mathbf{U}_{R_B} and \mathbf{U}_o can be directly measured in experiment. To IWPT system in air, there is no eddy current loss and $R_{eddy} = 0$.

Through two-coil circuit model involving EECLI, theoretical value of output voltage can be obtained using numerical software Wolfram Mathematica.

III. EXPERIMENT RESULTS AND ANALYSIS

In order to further analyze the output characteristics and EECLI variation of WPT in seawater, an experiment is carried out in air and seawater separately. The experiment and calculation results in different conditions are compared and analyzed to verify the correctness of theoretic model mentioned in the previous section.

A. Experimental Setup and Procedure

In this case, the power source is set as AC voltage of which peak-peak value (PPV) is 15.4 V with operation frequency ranging from 300 kHz to 1 MHz. In the term of Tx and Rx coils, outer and inner diameter of the 15-turn planar spiral coils wound by litze wire of 1.2 mm diameter are 8 cm and 12 cm respectively, as shown in Fig. 3. The self inductance of Tx and Rx coils are about 10.2 and 10.4 μH measured by LCR meter (GW Instek:LCR821)

with 200 kHz frequency. Both two sides adopt 7.6 nF capacitor to achieve resonant frequency around 570 kHz. In order to improve the quality factor of the circuit and observe frequency splitting phenomenon, the external resistors in Tx and Rx are set as 5 Ω.



Fig. 3: Spiral coil

To imitate IWPT under seawater environment, the coils are put into a 25*20*15 cm water tank made of acrylic board and containing 13 cm high water level fully submerging two coils. Meanwhile, the conductivity of salt water is approximately 4.1 S/m measured by conductivity meter (LICHEN LC-DDB-1A), which is nearly same as seawater. The complete experimental setup is demonstrated in Fig. 4, which is composed of a signal generator (Tektronix: AFG3102) feeding sinusoidal signals to a 10 W power amplifier (Rigol: PA1011), water tank, IWPT circuit prototype and oscilloscope (RIGOL DS4014) utilized to illustrate waveform of voltage on resistors in Tx and Rx. More specific parameters of IWPT circuit protocol is illustrated in Table. 1, while the experimental procedure is shown after.

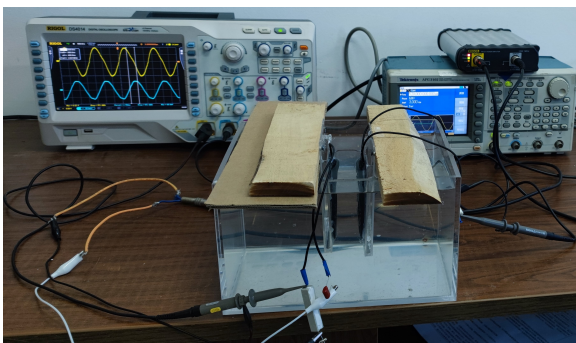


Fig. 4: IWPT experimental setup

A..1 Self resonant frequency determination

First, without the receiving side, Tx coil is put into air and the peak value of voltage on resistor is recorded with the frequency to determine the actual value of the self resonant frequency.

Table 1: Circuit parameters

| Components | Parameters | Values |
|------------|------------|---------|
| Tx | R_B | 5.00 Ω |
| | r_1 | 0.3 Ω |
| | C_1 | 7.71 nF |
| | L_1 | 10.2 μH |
| Rx | R_L | 5.02 Ω |
| | r_2 | 0.28 Ω |
| | C_2 | 7.66 nF |
| | L_2 | 10.4 μH |

A..2 Output voltage measurement on both sides

Next adding second side, the waveform of voltage on resistors in two sides is measured with various coil distance and sweeping frequency. The frequency step is 10 kHz and distance step is 0.5 cm. The experiment is carried out in air and salt water to investigate seawater ECL effects on WPT transmission characteristics. In this case, coil misalignment is not involved to simplify analysis procedure, therefore Tx coil is fixed while Rx coil is moved coaxially with Tx coil.

A..3 Determination of EECLI coefficient

In this case, EECLI coefficient β is determined as 6.5×10^{-5} by fitting to one experiment value arbitrarily.

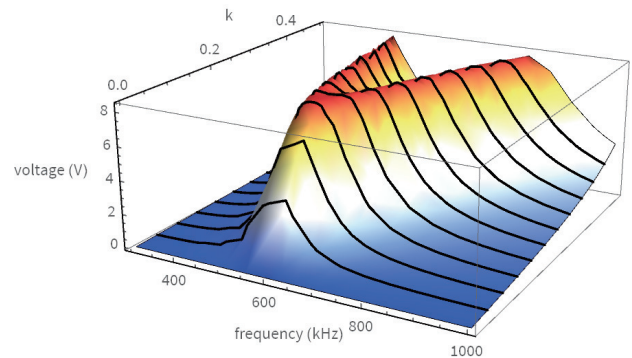


Fig. 5: Output voltage versus frequency and coupling coefficient, where the black lines are measured data and the continuous surface is theoretical values.

B. Experiment results

In the situation with merely first side, it is observed that the peak value of voltage on resistor appears near 570 kHz. When second side coupling with first side, Fig. 5 illustrates the relation in 3D among IWPT output voltage, frequency and coupling coefficient in seawater, which is obtained by model calculation and experiment, indicating that frequency splitting remains to exist [8].

The comparison between air and seawater is illustrated in Fig. 6. It is clear that frequency splitting phenomenon appears in both air and seawater to coils with diameter in centimeter level. Compared with IWPT

in air, seawater has a certain attenuation effect on output. In this case the splitting point emerges between 2 to 2.5 cm (around 0.15 converting to coupling coefficient). Specifically, there is no significant resonant frequency shifting observed, which corresponds to the theoretical model where seawater equivalent inductance value is relatively tiny as the IWPT coils are in small scale. On the other hand, as shown in Fig. 7, extracting output voltage on second side under resonant frequency, as the coil distance increases, both output voltage in air and seawater rises to the peak at splitting point, then decays to zero gradually. It is worth noting that EECLI mainly affects on the splitting ridge of the output, otherwise the influence is comparatively weak, which meets the calculation model as well. Furthermore, in order

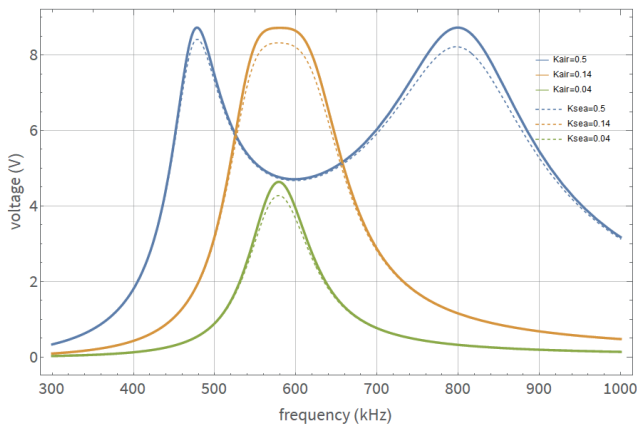


Fig. 6: Output voltage in air and seawater

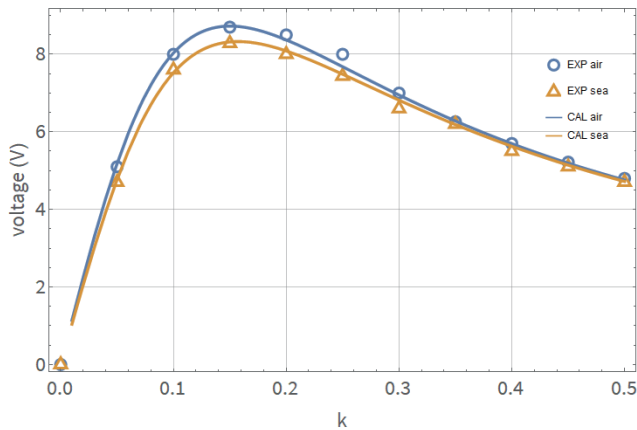
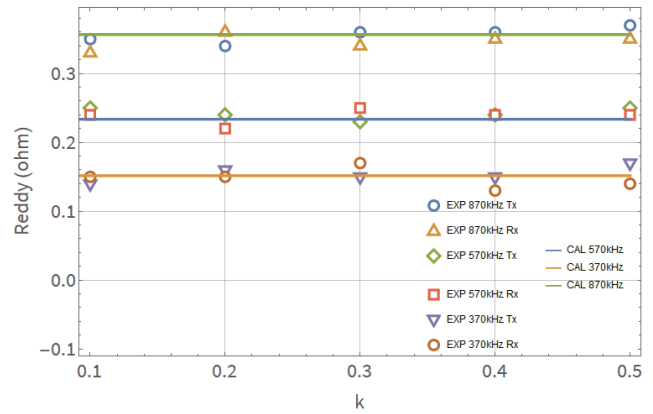


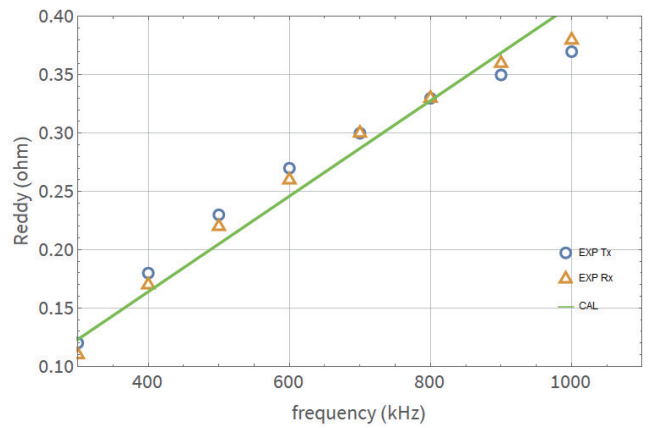
Fig. 7: Output voltage in air and seawater when resonance

to obtain the experimental value of EECLI in two sides, voltage value on resistors of two sides is recorded and substituted into (14).

Therefore, the experimental value of EECLI versus different coupling coefficient and frequency is obtained as shown in Fig. 8 (a) and (b), respectively, where the solid lines represent the calculation and the markers are the experiment values in Tx and Rx. Fig. 8 (a) illustrates the trends of EECLI value over coupling coefficient k



(a)



(b)

Fig. 8: EECLI variation: (a) EECLI value versus coupling coefficient k ; (b) EECLI value versus frequency

from 0.1 to 0.5 at resonant and non-resonant frequency (370 kHz, 570 kHz and 870 kHz, respectively). At 370 kHz, the mean EECLI values of Tx and Rx are 0.154 and 0.148 Ω close to calculation value 0.152 Ω . At 570 kHz, the average EECLI of primary and second side are 0.242 and 0.238 Ω which are consistent with the calculation value 0.234 Ω . Similarly at 870 kHz, the average EECLI of two sides are 0.356 and 0.346 Ω meeting the calculation value 0.357 Ω as well. It is noticeable that EECLI is independent to k , regardless of whether the system is in resonance or not.

Fig. 8 (b) demonstrates the relationship between EECLI and operation frequency from 300 kHz to 1 MHz. Specifically, EECLI presents a linear growth from approximately 0.1 to 0.4 Ω as frequency increases, where the experimental values conform to the calculation ones, which verifies the validity of (11). It is worth mentioning that comparing the outcome in this paper with the one by EMF method in [9], both shows positive correlation between EECLI and frequency, however quadratic relation is found in [9] and proportional relation is found in this study.

IV. CONCLUSIONS AND FUTURE WORK

In this paper, output characteristics of IWPT with coils in small size is analyzed via coupling circuit model containing EECLI, which is based on three-coil coupling model, instead of EMF model. Frequency splitting can be observed in IWPT under seawater as well as in air. The ECL mainly causes attenuation on the ridge of output. Most importantly, it is found that, for a symmetric system, EECL in two sides is equal and independent to coil distance, but proportional to operation frequency, which is similar to the conclusion by EMF model [9] and implies the significance of frequency optimization in the design of IWPT system in seawater. The proposed EECLI model omits the complex EMF calculation process and substantially improves the convenience of underwater IWPT analysis, while certain accuracy is ensured.

However, the relation between seawater resistance coefficient α and EECLI coefficient β is interesting to further discuss in the future. In addition, this paper is merely aimed at IWPT with coils in small dimension. The characteristics of IWPT with large-radius coils may differ [6] and will be more worth researching next step. Then, the practical application on large underwater devices such as UAVs with high power can be considered.

ACKNOWLEDGMENT

The authors would like to acknowledge their colleagues, for their assistant during the experiment.

REFERENCES

- [1] S. Lukic and Z. Pantic, "Cutting the cord: Static and dynamic inductive wireless charging of electric vehicles," *IEEE Electrification Magazine*, vol. 1, no. 1, pp. 57–64, 2013.
- [2] S. Y. R. Hui and W. W. C. Ho, "A new generation of universal contactless battery charging platform for portable consumer electronic equipment," *IEEE Transactions on Power Electronics*, vol. 20, no. 3, pp. 620–627, 2005.
- [3] Wonseok Lim, Jaehyun Nho, Byungcho Choi, and Taeyoung Ahn, "Low-profile contactless battery charger using planar printed circuit board windings as energy transfer device," in *2002 IEEE 33rd Annual IEEE Power Electronics Specialists Conference. Proceedings (Cat.No.02CH37289)*, vol. 2, pp. 579–584 vol. 2, 2002.
- [4] C. Anyapo and P. Intani, "Wireless Power Transfer for Autonomous Underwater Vehicle," *2020 IEEE PELS Workshop on Emerging Technologies: Wireless Power Transfer (WoW)*, Seoul, Korea (South), 2020, pp. 246–249.
- [5] Z. Liu, L. Wang, Y. Guo and C. Tao, "Eddy Current Loss Analysis of Wireless Power Transfer System for Autonomous Underwater Vehicles," *2020 IEEE PELS Workshop on Emerging Technologies: Wireless Power Transfer (WoW)*, Seoul, Korea (South), 2020, pp. 283–287.
- [6] W. Niu, W. Gu and J. Chu, "Experimental investigation of frequency characteristics of underwater wireless power transfer," *2018 IEEE MTT-S International Wireless Symposium (IWS)*, Chengdu, China, 2018, pp. 1–3.
- [7] A. Askari, R. Stark, J. Curran, D. Rule, and K. Lin, "Underwater wireless power transfer," in *2015 IEEE Wireless Power Transfer Conference (WPTC)*, pp. 1–4, 2015.
- [8] W. Niu, J. Chu, W. Gu and A. Shen, "Exact Analysis of Frequency Splitting Phenomena of Contactless Power Transfer Systems," in *IEEE Transactions on Circuits and Systems I: Regular Papers*, vol. 60, no. 6, pp. 1670–1677, June 2013.
- [9] K.-H. Zhang, Z.-B. Zhu, L.-N. Du, and B.-W. Song, "Eddy loss analysis and parameter optimization of the WPT system in seawater," *Journal of Power Electronics*, vol. 18, no. 3, pp. 778–788, 2018.
- [10] K. Zhang, Y. Ma, Z. Yan, Z. Di, B. Song, and A. P. Hu, "Eddy current loss and detuning effect of seawater on wireless power transfer," *IEEE Journal of Emerging and Selected Topics in Power Electronics*, vol. 8, no. 1, pp. 909–917, 2020.
- [11] Z. Yan, B. Song, K. Zhang, H. Wen, Z. Mao, and Y. Hu, "Eddy current loss analysis of underwater wireless power transfer systems with misalignments," *AIP Advances*, vol. 8, no. 10, p. 101421, 2018.
- [12] Z. Yan, Y. Zhang, T. Kan, F. Lu, K. Zhang, B. Song, and C. C. Mi, "Frequency optimization of a loosely coupled underwater wireless power transfer system considering eddy current loss," *IEEE Transactions on Industrial Electronics*, vol. 66, no. 5, pp. 3468–3476, 2019.
- [13] L. U. Daura, G. Tian, Q. Yi, and A. Sophian, "Wireless power transfer-based eddy current non-destructive testing using a flexible printed coil array," *Philosophical Transactions of the Royal Society A*, vol. 378, no. 2182, p. 20190579, 2019.
- [14] B. Song, and C. C. Mi, "A new coil structure to reduce eddy current loss of WPT systems for underwater vehicles," *IEEE Transactions on Vehicular Technology*, vol. 68, no. 1, pp. 245–253, 2019.
- [15] C. Ye, O. Postolache, Y. Yang and W. Niu, "Design of Wireless Power Transfer Circuit for Stable Voltage Output," *2020 International Conference and Exposition on Electrical And Power Engineering (EPE)*, Iasi, Romania, 2020, pp. 709–714.
- [16] Kuan-Wei Wu, Mansour Karkoub, Tzu-Sung Wu "Robust Adaptive Fuzzy Control Design for 3-D Tower Crane with Time Delayed States", pp.26-33, vol. 2, 2020, *International Journal of Electrical Engineering and Computer Science (EEACS)*.
- [17] D. Barth, I. A. Gorchach, G. Gruhler, "Modelling of a Thermal Spraying Controller Using MATLAB/Simulink", pp.79-84, vol. 2, 2020, *International Journal of Electrical Engineering and Computer Science (EEACS)*.
- [18] Pardeep Kumar, Hari Mohan, G. A. Hoshoudy, "FLR Effect on Stability of a Plasma in Porous

Medium” pp.90-97, vol. 2, 2020, International Journal of Electrical Engineering and Computer Science (EEACS).

W. Niu received the B.E. degree from Xi’an Aerotechnical College, Xi’an, China, in 1998, the M.E. degree from Northwestern Polytechnical University, Xi’an, in 2004, and the Ph.D. degree from Shanghai Jiao Tong University, Shanghai, China, in 2008.

From 2013 to 2014, he was a Visiting Lecturer with McMaster University, Hamilton, ON, Canada. Since 2008, he has been a Lecturer with Shanghai Maritime University, Shanghai, where he has been an Associate Professor, since 2017. His research interests include wireless power transfer, control of marine equipment, and prognostics and health management.

C. Ye received the B.E. degree from Shanghai Maritime University, Shanghai, China, in 2016. He is currently pursuing the M.S. degree with Shanghai Maritime University, Shanghai, China.

His main research interest includes wireless power transfer technology.

W. Gu received the B.E. and Ph.D. degrees from Shanghai Maritime University, Shanghai, China, in 1982 and 2008, respectively.

Since 1982, he has been a Teacher with Shanghai Maritime University, where he has been a Professor, since 1997, and is currently the Director of the Key Laboratory of Transport Industry of Marine Technology and Control Engineering. His research interest includes marine information control technology.

Contribution of individual authors to the creation of a scientific article (ghostwriting policy)

Wangqiang Niu did the study conceiving and methodology.

Chen Ye carried out the experiment and original draft preparation.

Wei Gu is responsible for review and editing.

In general, please, follow

<http://naun.org/main/format/contributor-role.pdf>

Creative Commons Attribution License 4.0 (Attribution 4.0 International, CC BY 4.0)

This article is published under the terms of the Creative Commons Attribution License 4.0

https://creativecommons.org/licenses/by/4.0/deed.en_US